PRIFYSGOL BANGOR / BANGOR UNIVERSITY

PRIFYSGOL
BANGOR
UNIVERSITY

Choosing the correct strong correlation correction for U3Si2: influence of magnetism

Liu, Huan; Claisse, Antoine; Middleburgh, Simon; Olssen, Par

Journal of Nuclear Materials

DOI:
10.1016/j.jnucmat.2019.151828

Published: 15/12/2019

Peer reviewed version

Cyswllt i'r cyhoeddiad / Link to publication

Dyfyniad o'r fersiwn a gyhoeddwyd / Citation for published version (APA):
Liu, H., Claisse, A., Middleburgh, S., & Olssen, P. (2019). Choosing the correct strong correlation correction for U3Si2: influence of magnetism. *Journal of Nuclear Materials*, *527*, [151828]. https://doi.org/10.1016/j.jnucmat.2019.151828

Hawliau Cyffredinol / General rights
Copyright and moral rights for the publications made accessible in the public portal are retained by the authors and/or other copyright owners and it is a condition of accessing publications that users recognise and abide by the legal requirements associated with these rights.

• Users may download and print one copy of any publication from the public portal for the purpose of private study or research.
• You may not further distribute the material or use it for any profit-making activity or commercial gain
• You may freely distribute the URL identifying the publication in the public portal ?

Take down policy
If you believe that this document breaches copyright please contact us providing details, and we will remove access to the work immediately and investigate your claim.

06. May. 2023

Choosing the correct strong correlation correction for U_3Si_2: influence of magnetism

Huan Liu[1], Antoine Claisse[2], Simon C. Middleburgh[3], Pär Olsson[1,*]

[1]KTH Royal Institute of Technology, Nuclear Engineering, SE-100 44, Stockholm, Sweden
[2] Westinghouse Electric Sweden, SE-72163, Västerås, Sweden
[3]Bangor University, Nuclear Futures Institute, LL57 2DG, Bangor, Gwynedd

* Corresponding author. E-mail: polsson@kth.se

Abstract

Physical properties of U_3Si_2 with non-magnetic, ferromagnetic, and anti-ferromagnetic structures are predicted using DFT+*U* with Hubbard-*U* values from 0 to 4 eV. The stability of U_3Si_2 is compared with its neighboring phases, U_3Si and USi. The results emphasize the importance of magnetism. For non-magnetic U_3Si_2 a very large Hubbard-*U* value is required to accurately reproduce the physical constants. However, from the electronic structure of the studied magnetic states with different Hubbard-*U* values, it is clear that it is incorrect to use a non-magnetic model for paramagnetic U_3Si_2 because of the resulting nearly zero occupation of f-electrons.

Binary uranium silicide compounds, principally U_3Si_2, are receiving interest as potential accident tolerant or high-performance fuel candidates in commercial light water reactors (LWRs)[1] and have been employed in a number of test reactors globally. Possessing higher uranium density than canonical oxide fuel (U_3Si_2: 11.3 g(U)/cm^3[2], UO_2: 9.7 g(U)/cm^3[3]) and greatly improved thermal conductivity[4] implies that uranium silicide compounds are quite promising. The high fissile density implies better fuel economy or larger operational flexibility, while the excellent thermal conductivity could provide larger margins in certain postulated accidents owing to the larger power to melt ratio.

Density functional theory (DFT) has been used to investigate a number of material properties of U_3Si_2 relevant to fuel performance and the safe operation of the fuel in

reactor. Because of the failure of conventional DFT to properly describe strongly correlated uranium 5f-electons, the Hubbard-*U* correction has been employed. In previous work, the choices of Hubbard-*U* value for uranium of U_3Si_2 have differed. For example, Wang et al.[5] used U_{eff} = 4 eV by fitting to the U_3Si_2 lattice constants. Andersson[6] reported that the application of Hubbard-*U* would eliminate the structural distortion predicted by conventional DFT, but increase the unit cell volume. The best balance was achieved for U_{eff} = 1.5 eV. Noordhoek et al.[7] also indicated that U_{eff} = 1.5 eV was most appropriate, stabilizing the experimentally observed crystal structure while simultaneously stabilizing this structure compared to its observed neighboring phases. A number of subsequent studies have used the DFT+*U* parameters highlighted by Noordhoek et al.[7] to successfully predict other fuel performance relevant behaviors of U_3Si_2 [8–10].

A problem with the methodology proposed by Noordhoek et al.[7] (or by Andersson[6]) is that the stable magnetic structure predicted is ferromagnetic (or anti-ferromagnetic). The work of Miyadai et al.[11,12] has observed the system to be a Pauli paramagnet. Modelling a paramagnetic state ordering is more computationally complex and expensive[13–15] and considering paramagnetic systems as ferromagnetic or anti-ferromagnetic is more appropriate than removing spin-polarisation all together[16–19].

We here report the relationship between Hubbard-*U* value and lattice parameter, volume, and relative stability of U_3Si_2 based on non-spin, ferromagnetic, and anti-ferromagnetic state. The aim is to highlight the importance of the spin state on the choice of Hubbard-*U* value, and the correction effect.

DFT+*U* simulations are performed with the VASP package[20] applying the GGA-PBE[21] exchange correlation potential. The implementation of GGA+*U* applied is rotationally invariant introduced by Liechtenstein *et al.*[22] . Here an effective

Hubbard-U value, U_{eff} = (U - J) is used, J is set to zero. A plane-wave energy cut-off energy of 500 eV is employed for all calculations and the Methfessel-Paxton smearing method is used with an energy of 0.2 eV. The structure relaxations are based on a 2x2x2 supercell containing 80 atoms to allow for the distortion previously observed to appear, while the k-point grid is 4x4x8. The applied effective Hubbard-U value is varied from 0 to 4 eV. The anti-ferromagnetic state involved in this work is along the [001] direction. Unit cells are employed to study the formation energies of U_3Si_2 and of its neighboring phases, U_3Si with space group *Fmmm* and USi with space group *Pbnm*, and the k-point grids are chosen to be 8x8x16, 8x8x8, and 8x10x6 in order to match the k-point density across all systems. The formation energies of anti-ferromagnetic U_3Si_2 are calculated using a 1x1x2 supercell. The energy convergence criteria are set to 10^{-5} eV for 2x2x2 supercells, 10^{-6} eV for the unit cell and the 1x1x2 supercells.

The observed structure of U_3Si_2 has the tetragonal space group *P4/mbm*. The impact that a range of U values has on the lattice parameter a, a/c ratio, volume, and total energy of unit cell is calculated, and the results are displayed in Fig. 1. Comparing with the experimental measurements, the lattice parameters and volumes of the magnetic structures are significantly overestimated by DFT+U when the Hubbard-U value is higher than 1.5 eV. The a/c ratio of the anti-ferromagnetic structure is underestimated for U_{eff} lower than 1.5 eV. This structural distortion results from the fact that the (001) plane composed of both U and Si is split into two distinct layers, as illustrated in Fig. 2 (a) and (b). For the values of 1.5 eV or higher the structure relaxes back to the ideal U_3Si_2 structure (see Fig. 2 (c) and (d)). The total energies of the studied systems shown in the bottom of Fig.1 are normalized according to the reference state (U_{eff} = 0 for ferromagnetic order). One notes that for magnetic states, when a very large U_{eff} is applied (≥ 2.5 eV), the properties shown in Fig.1 are all saturated with respect to U_{eff}. This supports the probable existence of metastable states in that range. Fig. 3 shows the relationship between the local magnetic moment

of uranium atom and Hubbard-*U* value. It can be seen that the magnetic moment increases significantly with increasing U_{eff} for both ferro- and anti-ferromagnetic structures, but this trend is broken when U_{eff} is higher than 1.5 eV. This is because when U_{eff} increased from 0 to 1.5 eV, the Fermi energy decreases correspondingly and also the spin population. When U_{eff} is higher than 1.5 eV, the Fermi energy is independent of the U_{eff} value and the spin population stays largely unchanged. These results draw the same conclusion as previous work[6,7] that U_{eff} = 1.5 eV is most appropriate for both ferromagnetic and anti-ferromagnetic U_3Si_2. In the non-magnetic case, the calculated lattice constants and volume (a = 7.34 Å, c = 3.90 Å, V = 209.77 $Å^3$) closely match with the experimentally reported values (a = 7.33 Å, c = 3.90 Å, V = 209.63 $Å^3$ [23]) when U_{eff} = 4 eV.

The stability of the different magnetic states of U_3Si_2 are compared with U_3Si and USi, respectively, as reported in Fig. 4. The formation energy of binary U-Si compounds are calculated with respect to diamond-silicon and α-uranium for which the Hubbard-*U* term and spin states are consistent with the considered compound. In order to determine the ground state, the occupation matrix control scheme (OMC)[24] is employed for Hubbard-*U* values of 1.5 and 4.0 eV. The ferromagnetic and anti-ferromagnetic U_3Si_2 structures are on the convex hull for DFT+*U* (U_{eff} = 1.5 and 4.0 eV), but not standard DFT (U_{eff} = 0 eV) calculations. The non-magnetic U_3Si_2 structure is on the convex hull only when U_{eff} = 4.0 eV meaning that the achievement of the stability of non-magnetic ordering U_3Si_2 structure need a very large Hubbard-*U* value.

However, applying such a strong correlation correction to U_3Si_2 related studies requires extreme caution. DFT+*U* calculations with a too large Hubbard-*U* value would stop at a local minima rather than the global, e.g. the metastable state, resulting in unreliable predictions. Table 1 shows the initial diagonal matrices for U_3Si_2 and relative energies for different Hubbard-*U* values and magnetic states. The predicted

volume difference compared to experiments are also listed. Results of U_{eff} = 1.5 eV for the non-magnetic structure are not listed since the metastable states are completely absent. On one hand, the average energy difference between ground- and metastable states for U_{eff} = 4.0 eV in the non-magnetic structure is much higher than that of U_{eff} = 1.5 eV for magnetic structures. On the other hand, although applying a 4 eV Hubbard-*U* value to the non-magnetic structure can predict the crystal volume well in some cases, these states are energetically unstable.

Moreover, it is incorrect to consider the paramagnetic phase to be non-magnetic. Table 2 illustrates the energy differences between anti-ferromagnetic and ferromagnetic/non-magnetic configurations. The results are consistent with the calculations of Andersson et al.[25,26]. The small energy difference between different magnetic structures indicates that the structures with local magnetic moments on uranium atoms are more comparable with each other. Additionally, $\Delta E_{AFM\text{-}NM}$ (U_{eff} = 4 eV) in Table 2 are in the same order of some reported point defect formation energies[25], which shows that the difference between non-magnetic and paramagnetic structures will obstruct the point defect formation and migration investigations of paramagnetic U_3Si_2.

Fig. 5 shows the electronic density of states (DOS) of different magnetic states with different U_{eff}. For the ferro- and anti-ferromagnetic states (Fig.5 (c) to (f)), the spin-polarization degree of freedom allows for a minimum total DOS at the Fermi level when U_{eff} is 1.5 eV. This minimum originates from the f-orbital separation. For the non-magnetic states (Fig.5 (a) and (b)), not even high U_{eff} splits the f-orbital but shifts it to higher, unoccupied energies. However, the strong f-d hybridisation in the uranium atoms leads to a minimization of the total DOS at the Fermi level. The high Hubbard-*U* values applied for the non-magnetic simulations induces a near-zero occupation of f-electrons, which is clearly unreasonable. Accordingly, the employment of a 4 eV Hubbard-*U* value to non-magnetic U_3Si_2 is not physical.

In summary, the method of applying a 4 eV Hubbard-*U* value to non-magnetic U_3Si_2[5] structure has been shown to be unreliable. Our research highlights that consideration of the spin state is vital to the choice of *U* value even for a localized magnetic compound with low transition temperature like U_3Si_2. To model the paramagnetic structure in this simple method, spin polarized calculations must be considered but there is a clear scope for further work modelling the paramagnetic structure of U_3Si_2 in more depth.

Acknowledgment

The financial support by China Scholarship Council (No. 201700260222) is acknowledged. Simon C. Middleburgh is supported by the Sêr Cymru II programme funded through the Welsh European Funding Office (WEFO) under the European Development Fund (ERDF). This work was carried out as part of the CARAT programme investigating Accident Tolerant Fuels. The computations were performed on resources provided by the Swedish National Infrastructure for Computing (SNIC) at PDC, KTH. The authors greatfully acknowledge Boris Dorado at CEA/DAM, and Emerson Vathonne, Marjorie Bertolus and Michel Freyss at CEA/DEN for the development of a VASP version supporting the OMC framework.

References

[1] S.J. Zinkle, K.A. Terrani, J.C. Gehin, L.J. Ott, L.L. Snead, Accident tolerant fuels for LWRs: A perspective, J. Nucl. Mater. 448 (2014) 374–379. doi:10.1016/j.jnucmat.2013.12.005.

[2] J.T. White, A.T. Nelson, J.T. Dunwoody, D.D. Byler, D.J. Safarik, K.J. Mcclellan, Thermophysical properties of U 3 Si 2 to 1773 K, J. Nucl. Mater. 464 (2015) 275–280. doi:10.1016/j.jnucmat.2015.04.031.

[3] J.K. Fink, Thermophysical properties of uranium dioxide, J. Nucl. Mater. 279 (2000) 1–18. doi:10.1016/S0022-3115(99)00273-1.

[4] A. Berche, C. Rado, O. Rapaud, C. Guéneau, J. Rogez, Thermodynamic study of the U–Si system, J. Nucl. Mater. 389 (2009) 101–107. doi:10.1016/j.jnucmat.2009.01.014.

[5] T. Wang, N. Qiu, X. Wen, Y. Tian, J. He, K. Luo, X. Zha, Y. Zhou, Q. Huang, J. Lang, S. Du, First-principles investigations on the electronic structures of U3Si2, J. Nucl. Mater. 469 (2016) 194–199. doi:10.1016/j.jnucmat.2015.11.060.

[6] A. David Ragnar, Density functional theory calculations of defect and fission gas properties in U-Si fuels, 2016. https://permalink.lanl.gov/object/tr?what=info:lanl-repo/lareport/LA-UR-15-27996 (accessed January 25, 2019).

[7] M.J. Noordhoek, T.M. Besmann, D. Andersson, S.C. Middleburgh, A. Chernatynskiy, Phase equilibria in the U-Si system from first-principles calculations, J. Nucl. Mater. 479 (2016) 216–223. doi:10.1016/j.jnucmat.2016.07.006.

[8] S.C. Middleburgh, R.W. Grimes, E.J. Lahoda, C.R. Stanek, D.A. Andersson, Non-stoichiometry in U3Si2, J. Nucl. Mater. 482 (2016) 300–305. doi:10.1016/j.jnucmat.2016.10.016.

[9] S.C. Middleburgh, A. Claisse, D.A. Andersson, R.W. Grimes, P. Olsson, S. Mašková, Solution of hydrogen in accident tolerant fuel candidate material: U 3 Si 2, J. Nucl. Mater. 501 (2018) 234–237. doi:10.1016/j.jnucmat.2018.01.018.

[10] S.C. Middleburgh, P.A. Burr, D.J.M. King, L. Edwards, G.R. Lumpkin, R.W. Grimes, Structural stability and fission product behaviour in U 3 Si, J. Nucl. Mater. 466 (2015) 739–744. doi:10.1016/j.jnucmat.2015.04.052.

[11] T. Miyadai, H. Mori, Y. Tazuke, T. Komatsubara, Magnetic and electrical properties of the U-Si system, J. Magn. Magn. Mater. 90–91 (1990) 515–516. doi:10.1016/S0304-8853(10)80187-8.

[12] T. Miyadai, H. Mori, T. Oguchi, Y. Tazuke, H. Amitsuka, T. Kuwai, Y. Miyako, Magnetic and electrical properties of the U-Si system (part II), J. Magn. Magn. Mater. (1992). doi:10.1016/0304-8853(92)90697-M.

[13] V.I. Anisimov, A. V. Lukoyanov, Investigation of real materials with strong electronic correlations by the LDA+DMFT method, Acta Crystallogr. Sect. C Struct. Chem. 70 (2014) 137–159. doi:10.1107/S2053229613032312.

[14] I. Abrikosov, A. V Ponomareva, P. Steneteg, S.A. Barannikova, B. Alling, I.A. Abrikosov, P. Steneteg, B. Alling, Recent progress in simulations of the paramagnetic state of magnetic materials, (2015). doi:10.1016/j.cossms.2015.07.003.

[15] P. Steneteg, B. Alling, I.A. Abrikosov, Equation of state of paramagnetic CrN from *ab initio* molecular dynamics, Phys. Rev. B. 85 (2012) 144404. doi:10.1103/PhysRevB.85.144404.

[16] M. Ekholm, H. Zapolsky, A. V Ruban, I. Vernyhora, D. Ledue, I.A. Abrikosov, Influence of the magnetic state on the chemical order-disorder transition temperature in Fe-Ni prmalloy, Phys. Rev. Lett. 105 (2010). doi:10.1103/PhysRevLett.105.167208.

[17] V. Crisan, P. Entel, H. Ebert, ‡ H Akai, D.D. Johnson, J.B. Staunton, Magnetochemical origin for Invar anomalies in iron-nickel alloys, (n.d.). doi:10.1103/PhysRevB.66.014416.

[18] B. Alling, T. Marten, I.A. Abrikosov, Questionable collapse of the bulk modulus in CrN, Nat. Mater. 9 (2010) 283–284. doi:10.1038/nmat2722.

[19] A. V Smirnov, W.A. Shelton, D.D. Johnson, Importance of thermal disorder on the properties of alloys: Origin of paramagnetism and structural anomalies in bcc-based Fe 1−x Al x, (n.d.). doi:10.1103/PhysRevB.71.064408.

[20] G. Kresse, J. Furthmüller, Efficiency of ab-initio total energy calculations for metals and semiconductors using a plane-wave basis set, Comput. Mater. Sci. 6 (1996) 15–50. doi:10.1016/0927-0256(96)00008-0.

[21] P.E. Blöchl, Projector augmented-wave method, Phys. Rev. B. 50 (1994) 17953–17979. doi:10.1103/PhysRevB.50.17953.

[22] A.I. Liechtenstein, V.I. Anisimov, J. Zaanen, Density-functional theory and strong interactions: Orbital ordering in Mott-Hubbard insulators, Phys. Rev. B. 52 (1995) 15. doi:10.1103/PhysRevB.52.R5467.

[23] K. Remschnig, T. Le Bihan, H. Noël, P. Rogl, Structural chemistry and magnetic behavior of binary uranium silicides, J. Solid State Chem. 97 (1992) 391–399. doi:10.1016/0022-4596(92)90048-Z.

[24] B. Dorado, B. Amadon, M. Freyss, M. Bertolus, DFT+ U calculations of the ground state and metastable states of uranium dioxide, (2009). doi:10.1103/PhysRevB.79.235125.

[25] D.A. Andersson, X.-Y. Liu, B. Beeler, S.C. Middleburgh, A. Claisse, C.R. Stanek, Density functional theory calculations of self- and Xe diffusion in U3Si2, J. Nucl. Mater. 515 (2019) 312–325. doi:10.1016/j.jnucmat.2018.12.021.

[26] D.A. Andersson, X.Y. Liu, B. Beeler, S.C. Middleburgh, A. Claisse, C.R. Stanek, Corrigendum to “Density functional theory calculations of self- and Xe diffusion in U_3Si_2” [J. Nucl. Mater. 515 (2019) 312–325] (S0022311518311541)(10.1016/j.jnucmat.2018.12.021), J. Nucl. Mater. 518 (2019) 462–465. doi:10.1016/j.jnucmat.2019.03.038.

Table 1

Metastable states of non-magnetic (NM), ferromagnetic (FM) and anti-ferromagnetic (AFM) U_3Si_2 for different Hubbard-*U* values and for different initial diagonal occupation matrices. Symmetry is unconstrained in all cases. ΔE is the energy difference between metastable and ground-state in eV per uranium atom. $\Delta V/V_0$ is the difference between the calculated and experimental unit cell volume in %. V_0 represents the experimental value. The one marked with * is calculated using a 1x1x2 supercell. NM (U_{eff} = 1.5 eV) results are not listed because no metastable state exits in this situation.

	NM (U_{eff}=4.0 eV)		FM (U_{eff}=1.5 eV)		FM (U_{eff}=4.0 eV)		FM (U_{eff}=1.5 eV)*		AFM (U_{eff}=1.5 eV)*		AFM (U_{eff}=4.0 eV)*	
Initial matrix	ΔE	$\Delta V/V_0$	ΔE	$\Delta V/V_0$	ΔE	$\Delta V/V_0$	ΔE	$\Delta V/V_0$	ΔE	$\Delta V/V_0$	ΔE	$\Delta V/V_0$
0010010	0.639	0.052	0.065	6.750	0.236	12.174	0.002	7.155	0.000	7.239	0.035	12.648
0000011	0.227	8.071	0.052	7.098	0.276	13.171	0.002	7.141	0.001	7.053	0.031	12.520
0100100	0.000	9.684	0.000	7.165	0.000	12.622	0.000	6.540	0.001	6.974	0.004	12.634
0100001	0.000	9.684	0.000	6.511	0.082	12.789	0.000	6.371	0.014	6.848	0.010	12.827
0010100	0.748	0.525	0.126	6.206	0.252	12.322	0.001	7.053	0.000	7.198	0.248	12.773
0110000	0.000	9.684	0.059	6.573	0.260	38.134	0.000	6.349	0.014	6.888	0.000	12.560
1000100	0.844	-0.720	0.049	6.893	0.215	13.199	0.008	6.771	0.001	7.184	0.045	13.092
0000110	0.000	9.684	0.058	7.132	0.334	12.551	0.002	7.101	0.002	7.167	0.035	12.703
1100000	0.000	9.684	0.023	5.853	0.218	12.866	0.000	6.376	0.014	6.893	0.054	12.641
0001010	0.763	0.820	0.067	6.578	0.107	12.198	0.023	6.721	0.011	6.659	0.109	12.191
0001100	0.680	2.776	0.029	6.321	0.528	12.670	0.003	6.969	0.001	7.120	0.041	12.811
0000101	0.632	0.067	0.018	5.915	0.153	12.284	0.011	6.957	0.000	7.172	0.096	13.056
1010000	0.613	5.543	0.051	6.335	0.153	12.403	0.000	6.457	0.011	6.893	0.105	13.087
1000010	0.140	7.881	0.039	5.872	0.312	12.012	0.002	6.993	0.016	6.318	0.032	12.648
1000001	0.693	1.045	0.035	3.811	0.101	12.121	0.002	7.036	0.007	6.397	0.020	12.713
0001001	0.658	0.639	0.028	6.793	0.031	13.257	0.011	6.473	0.003	7.232	0.024	12.679
0011000	0.659	3.840	0.063	6.325	0.246	12.055	0.002	7.058	0.002	7.098	0.043	12.517
0100010	0.552	3.325	0.068	7.337	0.236	13.023	0.013	6.695	0.011	6.798	0.235	12.114
1001000	0.658	0.639	0.029	6.588	0.031	12.784	0.029	6.507	0.008	6.426	0.052	12.892
0010001	0.772	0.410	0.042	6.235	0.153	13.204	0.013	6.702	0.029	7.425	0.040	13.066
0101000	0.567	2.795	0.052	6.311	0.083	12.412	0.004	6.449	0.002	7.079	0.084	11.871
Average	0.469	4.101	0.045	6.410	0.191	13.821	0.006	6.756	0.007	6.955	0.064	12.669

Table 2

The energy difference (ΔE) between non-magnetic (NM) or ferromagnetic (FM) and anti-ferromagnetic (AFM) structures in eV/atom for different Hubbard-*U* values.

U_{eff}	0 eV	1.5 eV	4.0 eV
NM-AFM	0.049	0.172	0.636
FM-AFM	0.043	0.010	0.001

Figure captions

Fig. 1. The lattice parameter *a*, *a*/*c* ratio, volume, and total energy of unit U_3Si_2 cell in different magnetic states predicted with varying *U* values in GGA+*U*. The ferromagnetic structure with U_{eff} = 0 is chosen as reference state. The experimental vales are shown by the dashed lines.

Fig. 2. The relaxed structure of the (FM, AFM, NM) 2×2×2 U_3Si_2 supercell view in b-c for different *U*-values.

Fig. 3. The average local magnetic moment of uranium atoms of ferromagnetic (black) and anti-ferromagnetic (red) U_3Si_2 in μ_B predicted with different *U* values in GGA+*U*. The dashed lines are the mean values when U_{eff} is higher than 1.5 eV.

Fig. 4. The convex hull for ferromagnetic (top), anti-ferromagnetic (middle), and non-magnetic (bottom) U_3Si_2, U_3Si, and USi using DFT (U_{eff} = 0) and DFT+*U* (U_{eff} = 1.5, 4.0 eV) calculations.

Fig. 5. The electronic density of states for non-magnetic ((a) and (b)), ferromagnetic ((c) and (d)), and anti-ferromagnetic ((e) and (f)) U_3Si_2 with U_{eff} equal to 1.5 eV and 4.0 eV. The Fermi energy is set to zero. For (e) and (f) only half of the atoms are accounted for.

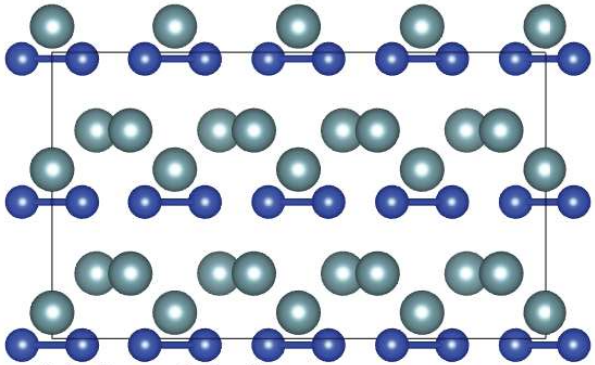

(a) U_{eff} = 0.0 eV

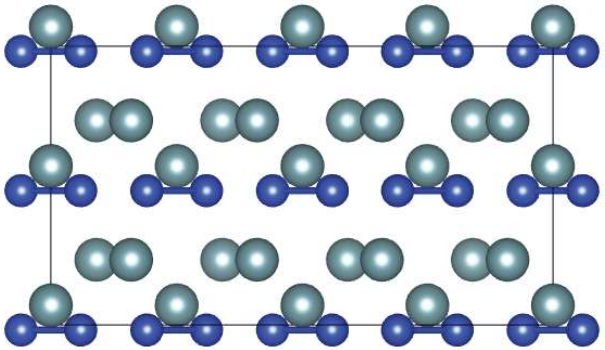

(b) U_{eff} = 1.0 eV

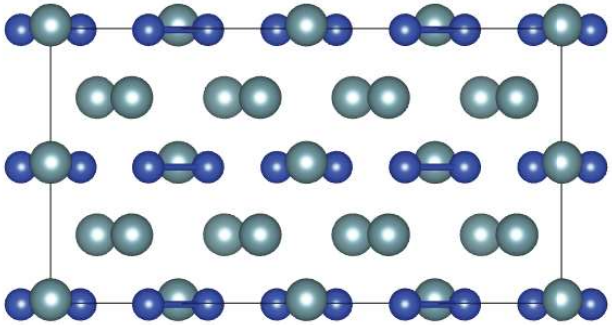

(c) U_{eff} = 1.5 eV

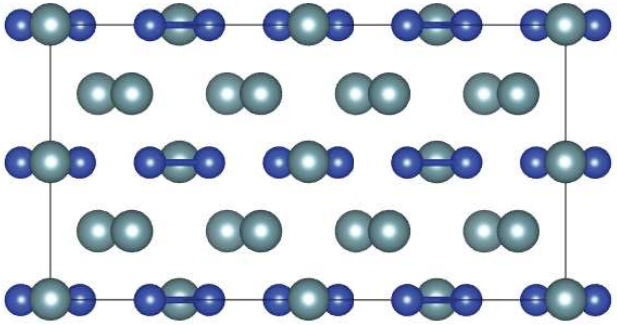

(d) U_{eff} = 2.0 eV

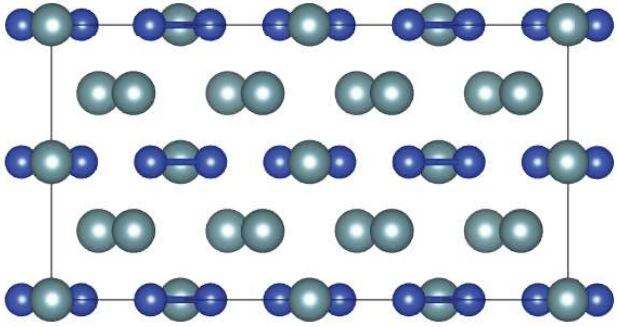

(e) Ideal stucture

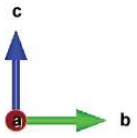

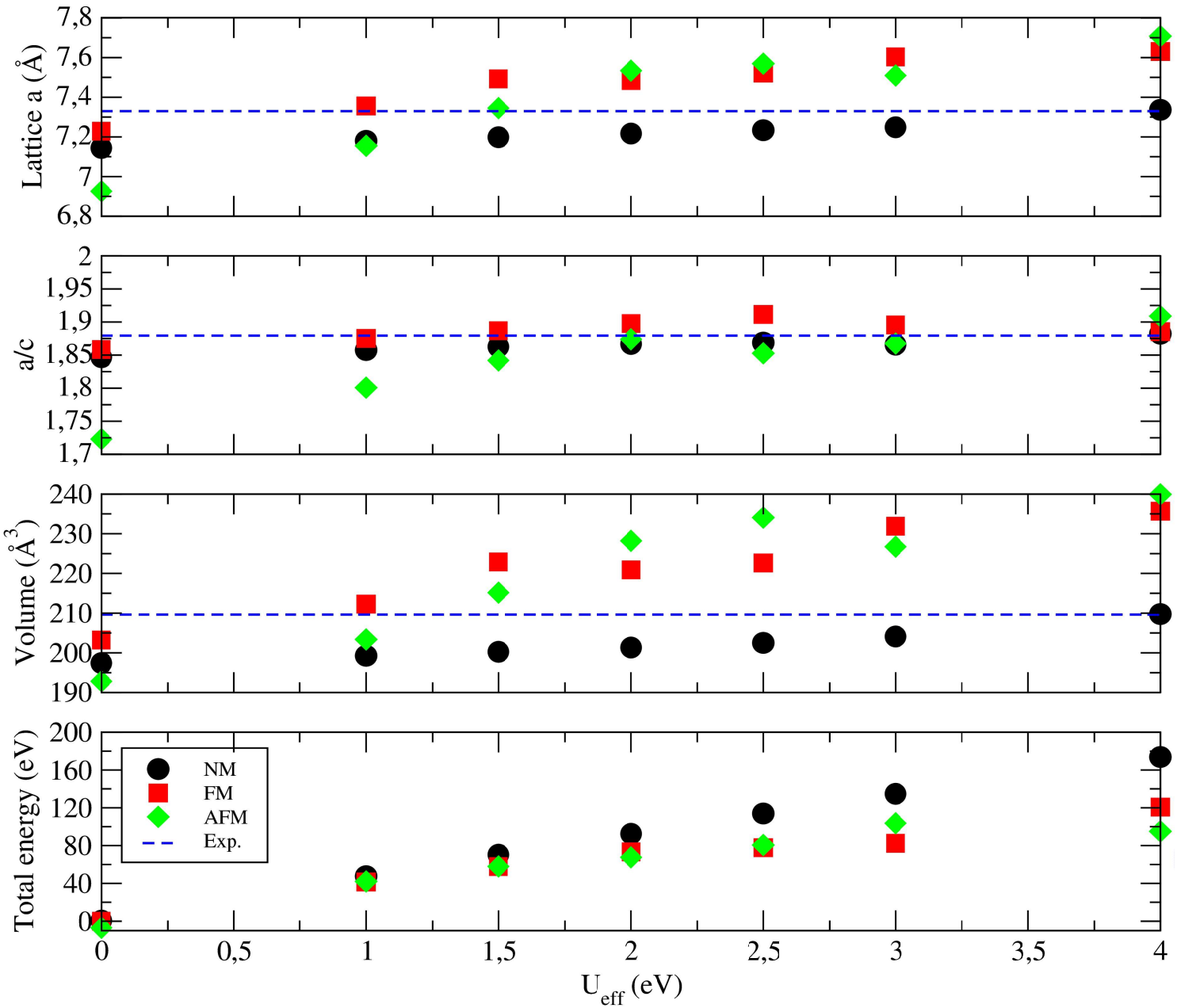
Lattice a (Å)
7,8
7,6
7,4
7,2
7
6,8
a/c
2
1,95
1,9
1,85
1,8
1,75
1,7
Volume (Å^3)
240
230
220
210
200
190
Total energy (eV)
200
160
120
80
40
0
NM
FM
AFM
Exp.
0
0,5
1
1,5
2
2,5
3
3,5
4
U_{eff} (eV)

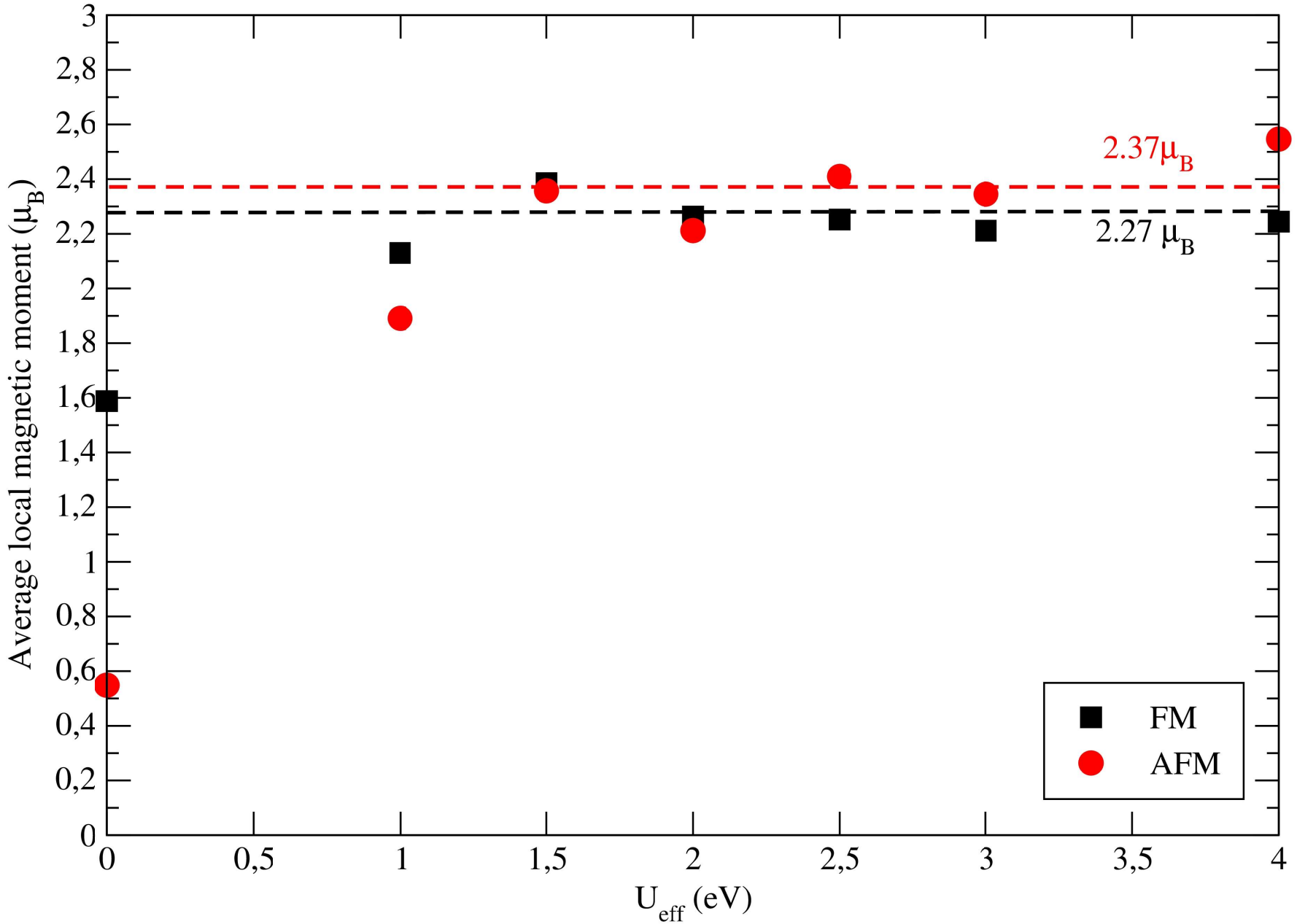
Average local magnetic moment (μ_B)
U_{eff} (eV)
2.37μ_B
2.27 μ_B
FM
AFM
0
0,2
0,4
0,6
0,8
1
1,2
1,4
1,6
1,8
2
2,2
2,4
2,6
2,8
3
0
0,5
1
1,5
2
2,5
3
3,5
4

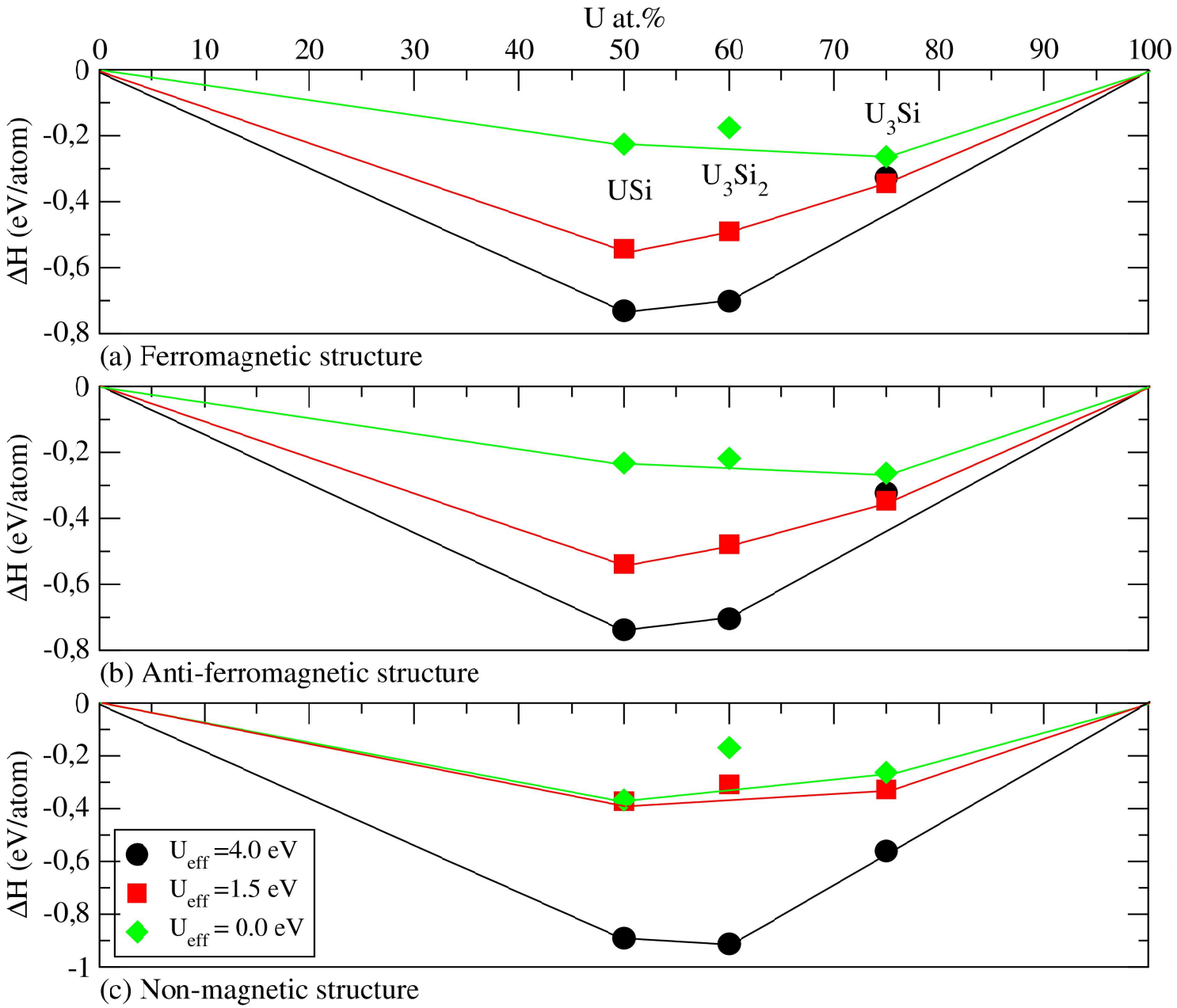
U at.%
0
10
20
30
40
50
60
70
80
90
100
ΔH (eV/atom)
0
-0,2
-0,4
-0,6
-0,8
USi
U3Si2
U3Si
(a) Ferromagnetic structure
(b) Anti-ferromagnetic structure
-1
Ueff =4.0 eV
Ueff =1.5 eV
Ueff = 0.0 eV
(c) Non-magnetic structure

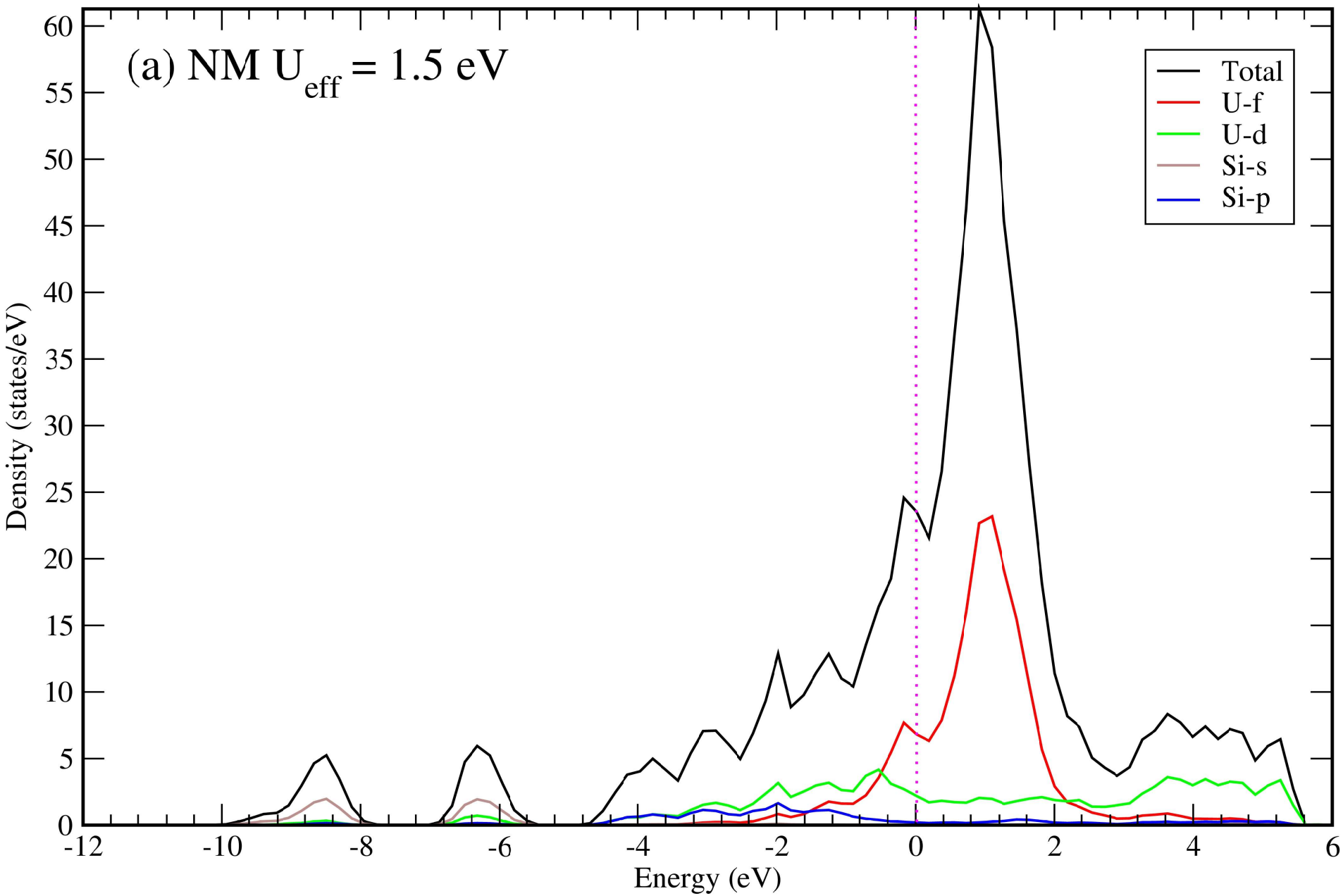
(a) NM U_eff = 1.5 eV
Total
U-f
U-d
Si-s
Si-p
Density (states/eV)
Energy (eV)
60
55
50
45
40
35
30
25
20
15
10
5
0
-12
-10
-8
-6
-4
-2
0
2
4
6

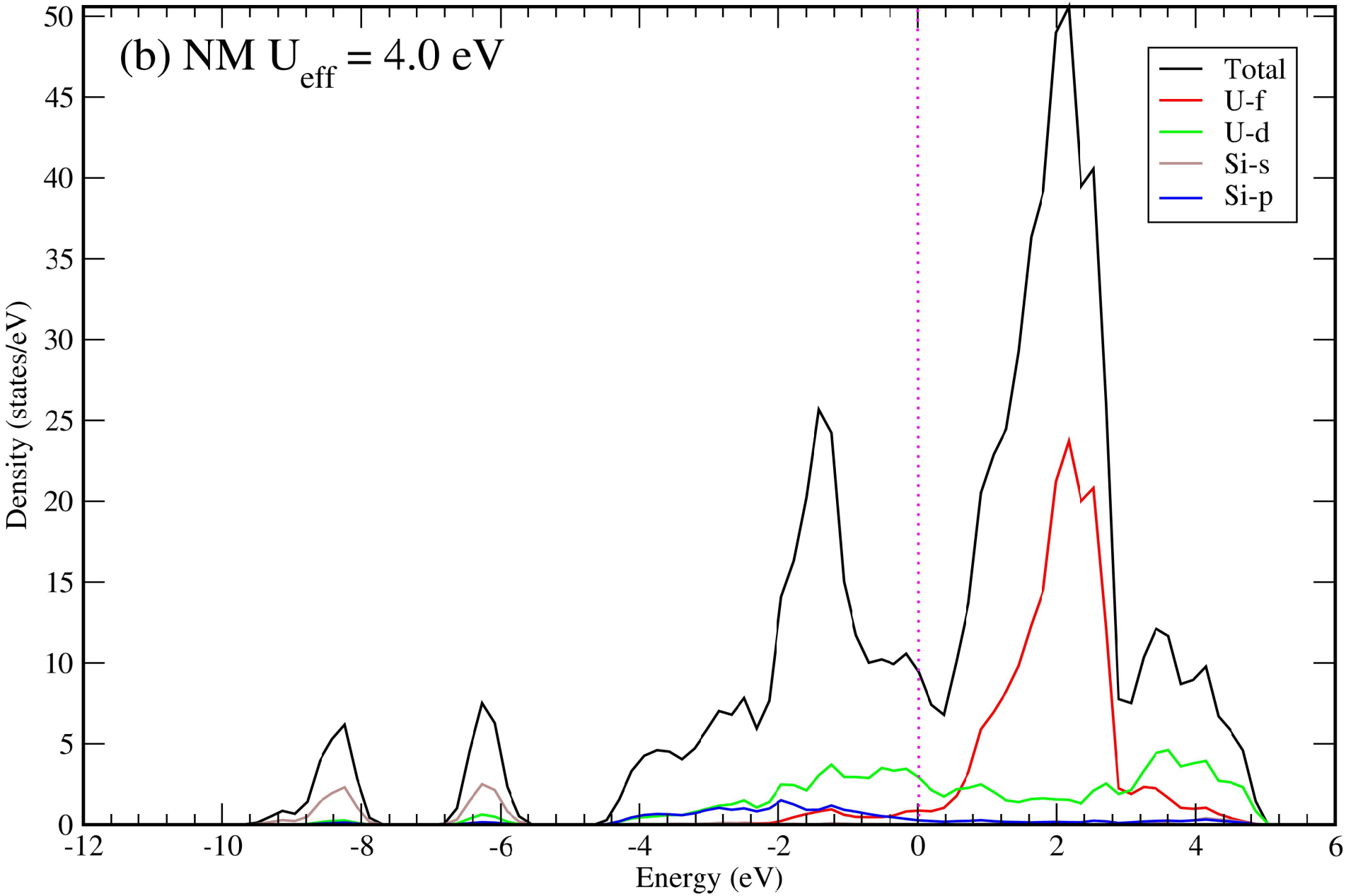
(b) NM U_eff = 4.0 eV
Total
U-f
U-d
Si-s
Si-p
Density (states/eV)
Energy (eV)
50
45
40
35
30
25
20
15
10
5
0
-12
-10
-8
-6
-4
-2
0
2
4
6

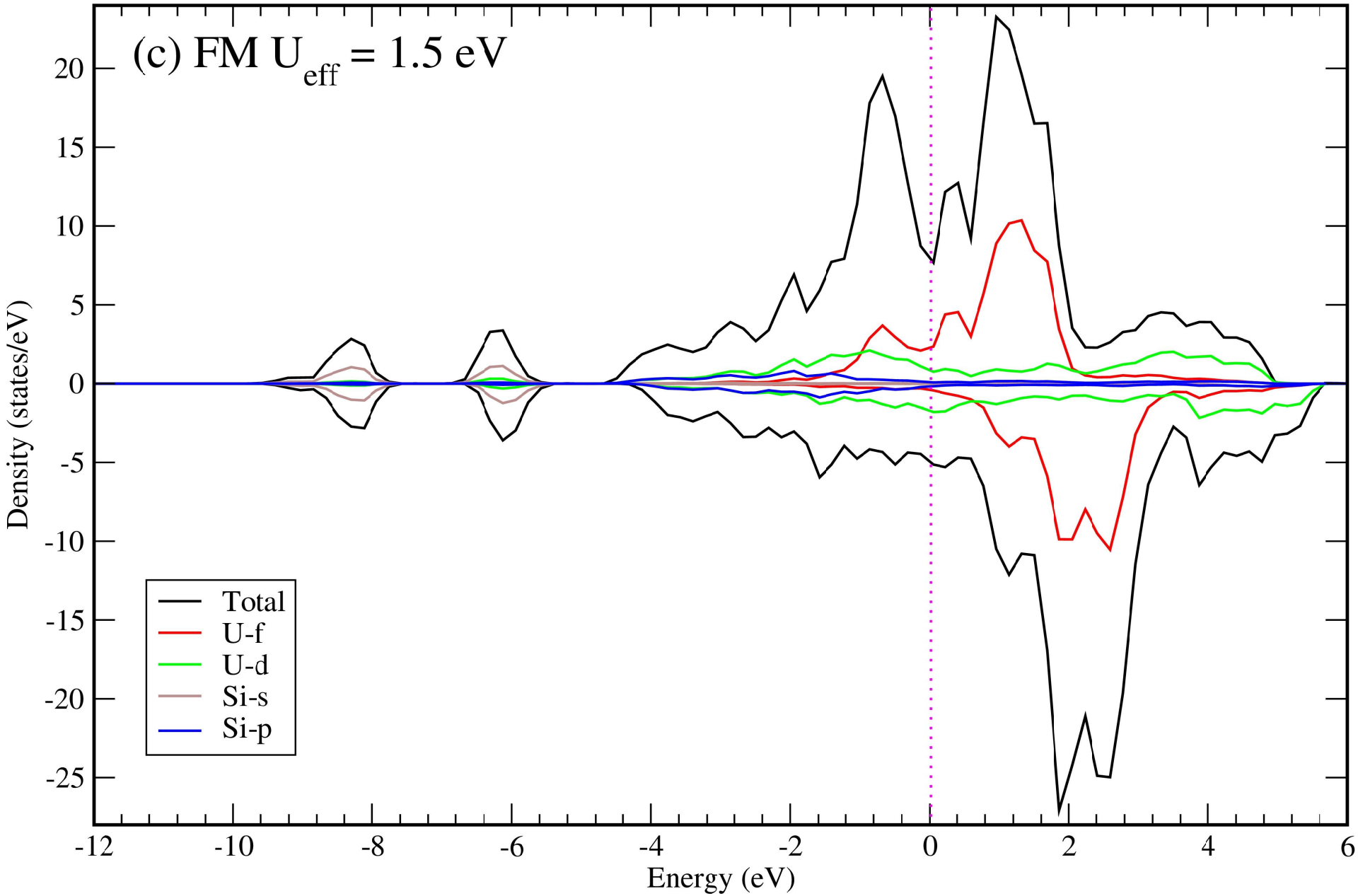
(c) FM U_eff = 1.5 eV
Density (states/eV)
Energy (eV)
Total
U-f
U-d
Si-s
Si-p
20
15
10
5
0
-5
-10
-15
-20
-25
-12
-10
-8
-6
-4
-2
0
2
4
6

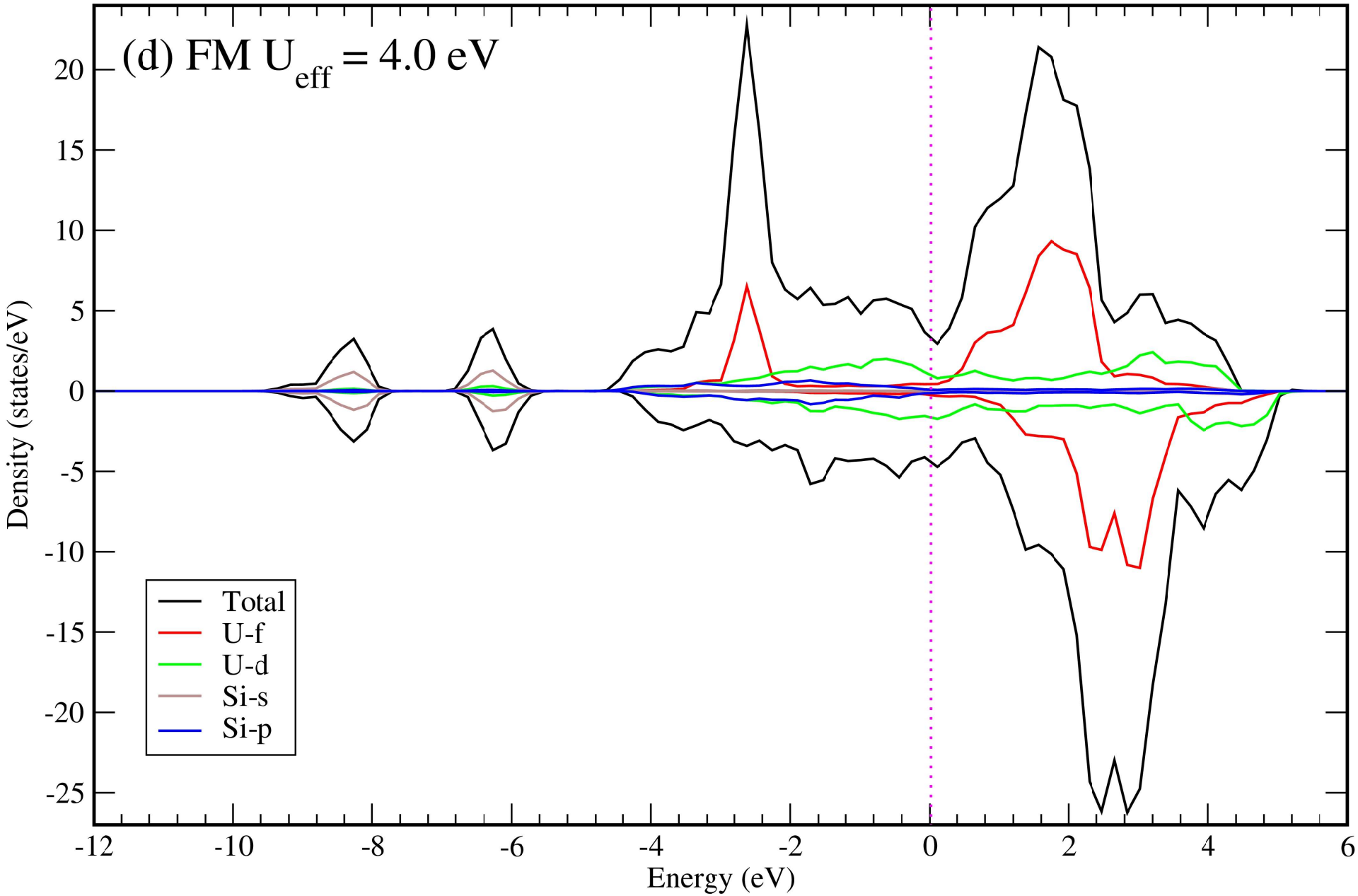
(d) FM U_eff = 4.0 eV
Density (states/eV)
Energy (eV)
Total
U-f
U-d
Si-s
Si-p
20
15
10
5
0
-5
-10
-15
-20
-25
-12
-10
-8
-6
-4
-2
0
2
4
6

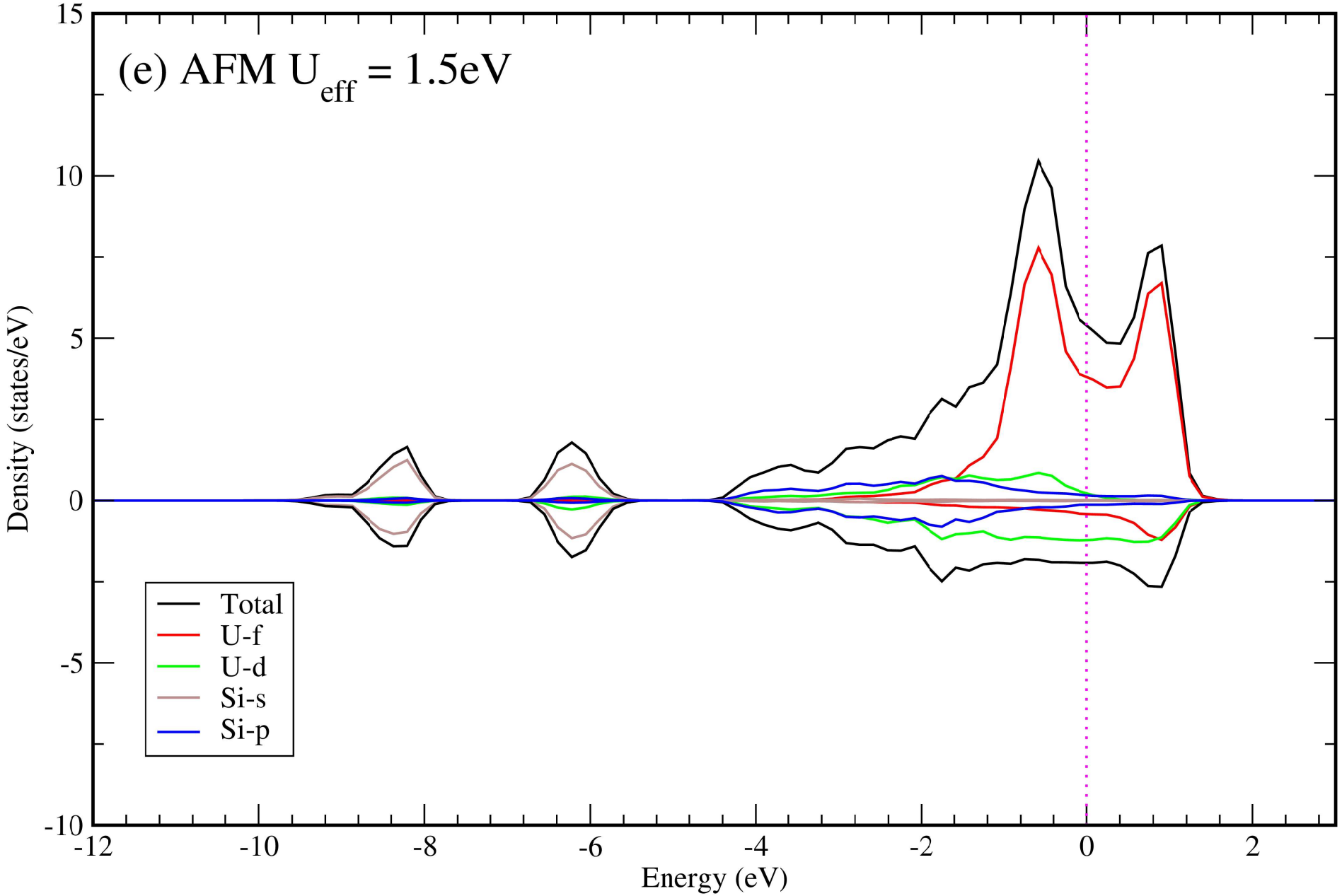
(e) AFM U_eff = 1.5eV
Density (states/eV)
Energy (eV)
15
10
5
0
-5
-10
-12
-10
-8
-6
-4
-2
0
2
Total
U-f
U-d
Si-s
Si-p

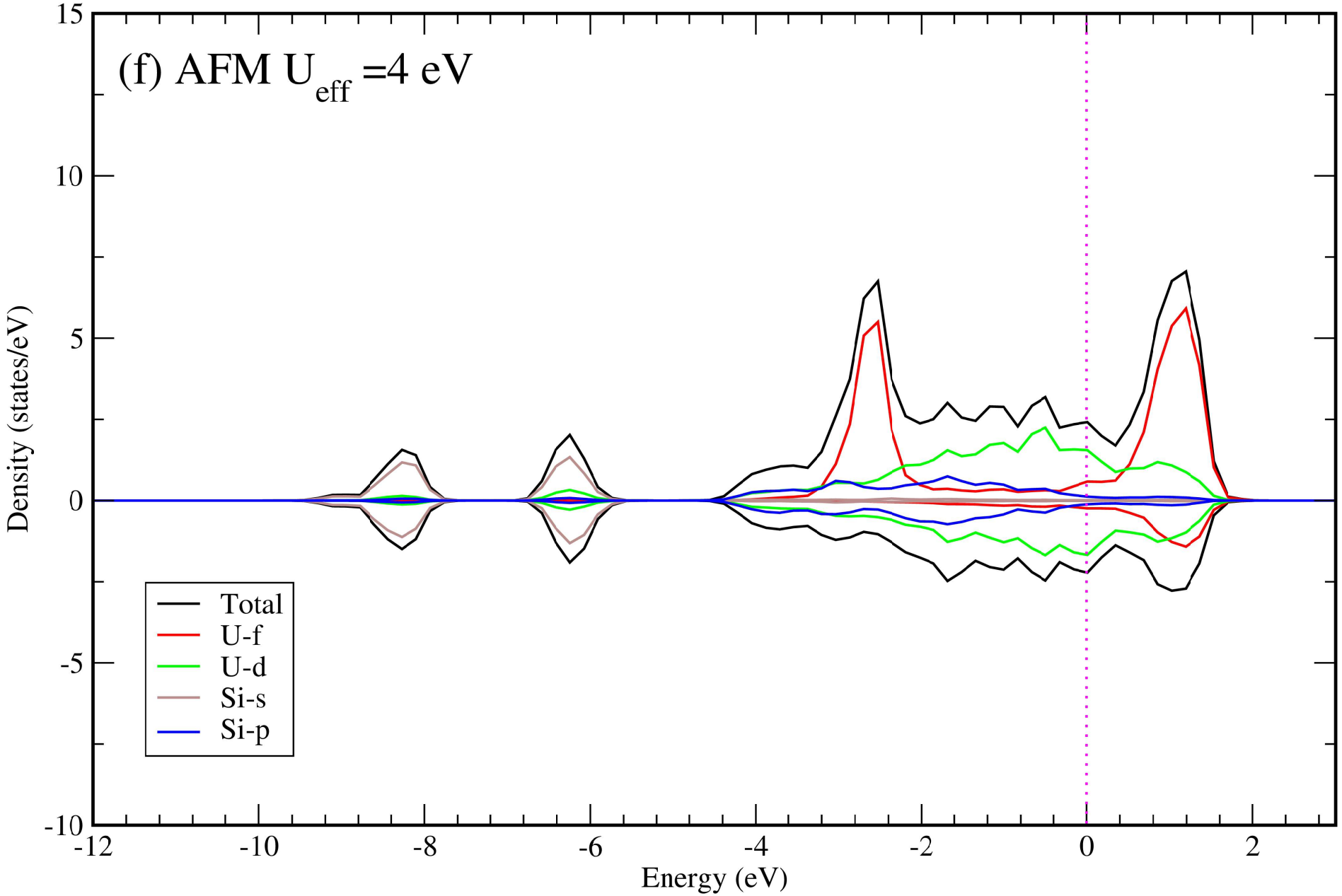
(f) AFM U_eff =4 eV
Density (states/eV)
Energy (eV)
Total
U-f
U-d
Si-s
Si-p
15
10
5
0
-5
-10
-12
-10
-8
-6
-4
-2
0
2